Electronic Supplementary Information

Supramolecular isomers: the first 3-fold interpenetrating 8-connected hex-c3 net and an unusual 4-fold interpenetrating $6^5.8$ net

Jin Yang,[a] Jian-Fang Ma,[a]* Stuart R. Batten,[b*] Seik Weng Ng[c], and Ying-Ying Liu[a]

[a] *Key Lab of Polyoxometalate Science, Department of Chemistry, Northeast Normal University, Changchun 130024, People's Republic of China*

[b] *School of Chemistry, Monash University, Victoria, 3800, Australia.*

[c] *Department of Chemistry, University of Malaya, 50603 Kuala Lumpur, Malaysia*

* Correspondence authors:
Prof. Jian-Fang Ma
E-mail: jianfangma@yahoo.com.cn
Fax: +86-431-8509-8620
Tel: *+86 431 85098620.*

Dr. Stuart R. Batten
E-mail: stuart.batten@sci.monash.edu.au
Fax: +61-3-9905-4597

Several typical 8-connected self-penetrating MOFs are listed below:

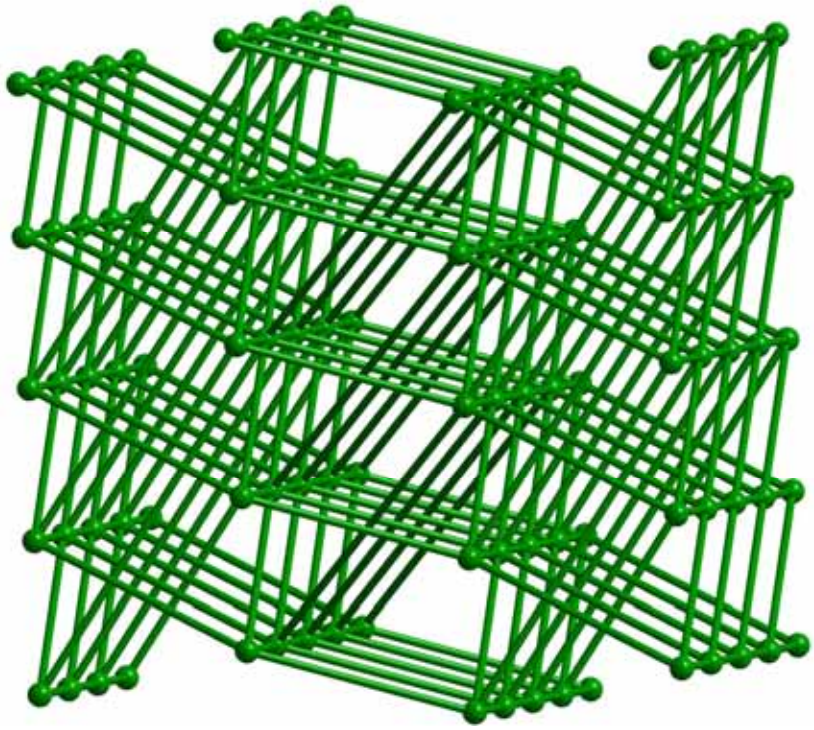

Fig. S1. The self-penetrating 8-connected $4^{20}6^8$ topology in $[Cd_3(bdc)_3(L)_2(H_2O)_2]$ (L = 1,4-bis(1,2,4-triazol-1-yl)butane and bdc = 1,4-benzenedicarboxylate). ***Chem. Eur. J.*, 2006, 12, 2680.**

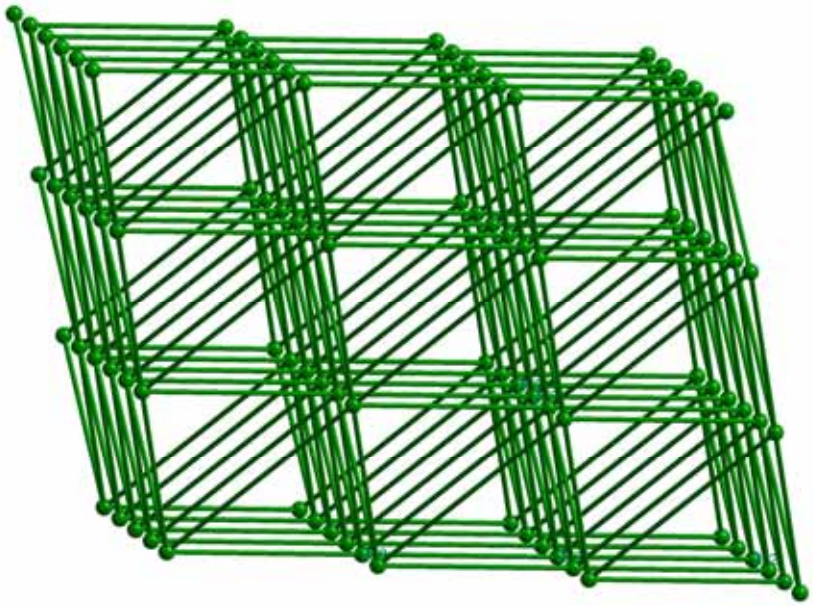

Fig. S2. The self-penetrating 8-connected $4^{24}56^3$ topology in $[Zn_5(OH)_2(bdc)_4(phen)_2]$ (phen = 1,10-phenanthroline and bdc = 1,4-benzenedicarboxylate). ***Chem. Commun.*, 2005, 4789.**

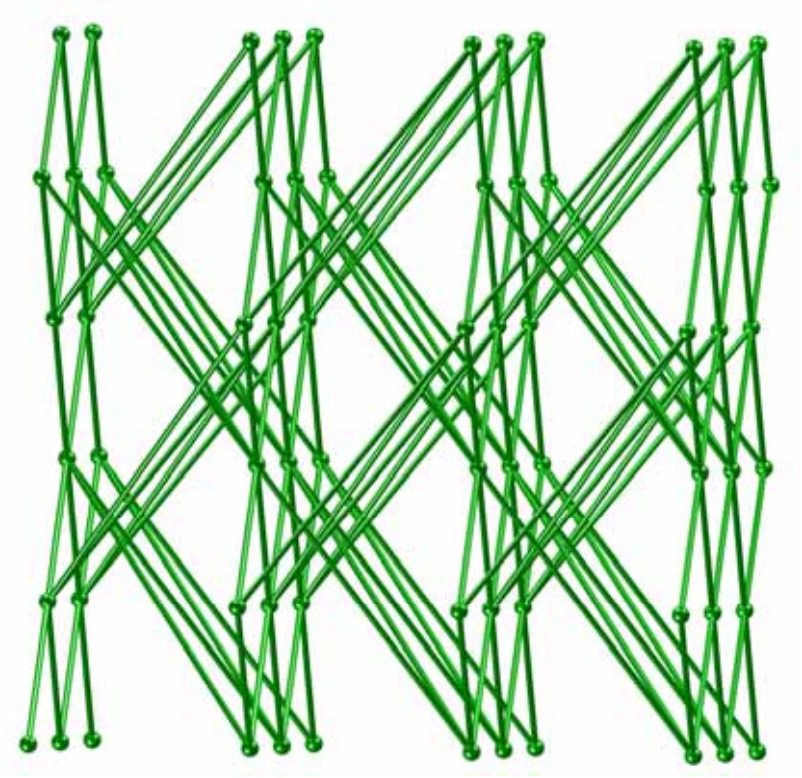

Fig. S3. The self-penetrating 8-connected $4^{16}6^{12}$ topology in $[Mn_4(L)_2(N_3)_8]_n$ (L = 1,3-bis(4-carboxylatopyridinium)propane). ***Inorg. Chem.*, 2009, 48, 789.**

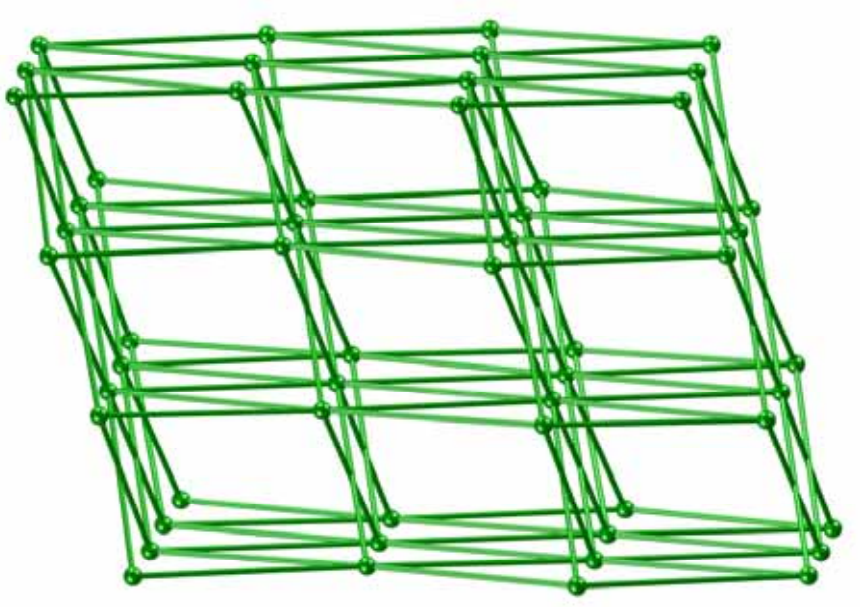

Fig. S4. The self-penetrating 8-connected $4^{24}6^4$ topology in $[Cu_4(bpp)_4V_4O_{12}]\cdot 3H_2O$ (bpp = 1,3-bis(4-pyridyl)propane) and $[Pb_6(\mu_4\text{-}O)_2(L)_4]_n$ (H_2L = 4,4'-(hexafluoroisopropylidene)bis-(benzoic acid)). ***Inorg. Chem.*, 2007, 46, 4775; *Cryst. Growth Des.*, 2010, 10, 2037.**

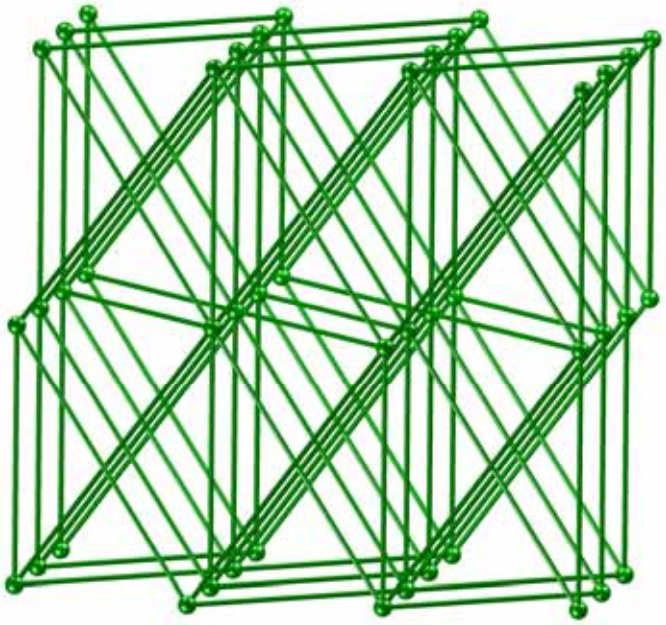

Fig. S5. The self-penetrating 8-connected $4^{16}6^{11}8$ topology in $[Zn_3(L^3)(oba)_3]$ (H_2oba = 4,4'-oxydibenzoic acid and L^3 = 1,4-bis[2-(2-pyridyl)imidazol-1-ylmethyl]benzene). ***Dalton Trans.*, 2008, 6796**.

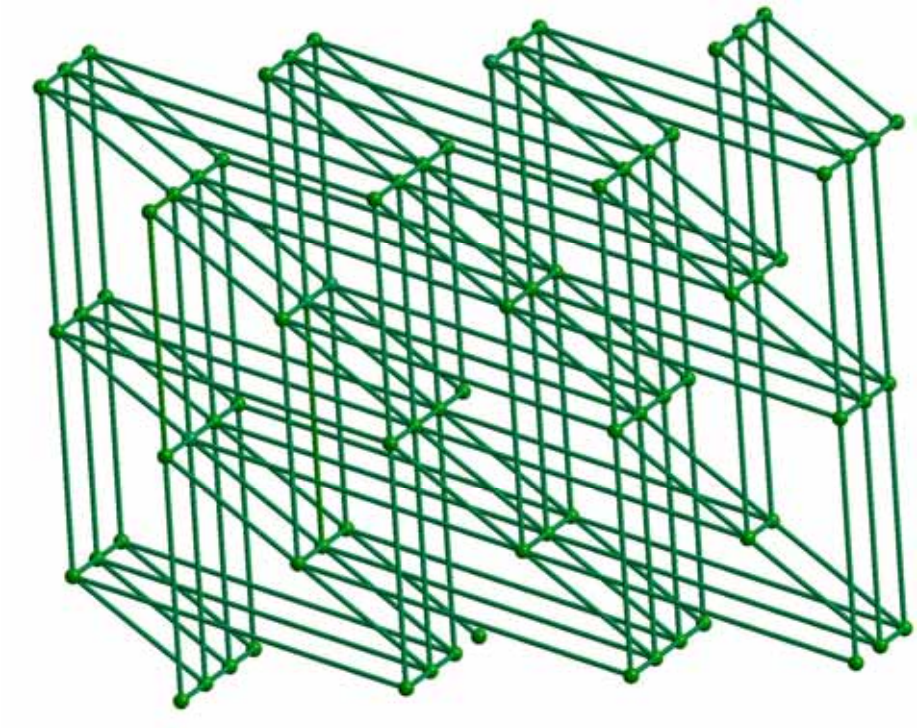

Fig. S6. The self-penetrating 8-connected $4^{16}5^{8}6^{4}$ topology in $[Co_3(ndc)_3(bbi)(CH_3CN)_2]$ (bbi = 1,1′-(1,4-butanediyl)bis(imidazole) and H_2ndc = 2,6-naphthalenedicarboxylic acid). ***Cryst. Growth Des.*, 2009, 9, 2756.**

Materials and Physical Measurements. All reagents and solvents for syntheses were purchased from commercial sources and used as received. The 1,2-bix was synthesized by following the procedures described previously (*J. Am. Chem. Soc.*, 1997, **119**, 2952). A solution containing imidazole (3.16 g, 46.4 mmol) and α,α′-dibromo-*o*-xylene (1.18 g, 4.46 mmol) in methanol (45 mL) was heated under reflux for 10 h. Removal of most of the solvent at reduced pressure gave a light yellow syrup which was dissolved in 100 mL of aqueous K_2CO_3 (6.13 g). This solution, upon standing, yielded crystalline of 1,2-bix, which was re-crystallized from water. The *trans*-azobenzene-4,4'-dicarboxylic acid dipotassium salt (K_2L) was prepared according to literature methods (*J. Polym. Sci. A: Polym. Chem.*, 1998, **36**, 2827). A warmed solution of α-D-glucose (10 g, 55.5 mmol) in water (40 mL) was added to a magnetically stirred solution of *p*-nitrobenzoic acid (1.3 g, 7.78 mmol), NaOH (5.0 g, 125 mmol), and water (25 mL) at 50°C over one hour period. A stream of air was vigorously bubbled into the light brown solution for 12 h with vigorous stirring, ultimately giving a dark brown mixture. On being cooled to room temperature, the mixture was slowly acidified with glacial acetic acid to pH = 6 and a precipitate was collected by filtration. Then, the solid was re-crystallized from hot aqueous K_2CO_3, yielding K_2L as bright orange needles. The C, H, and N elemental analyses were conducted on a Perkin–Elmer 240C elemental analyzer.

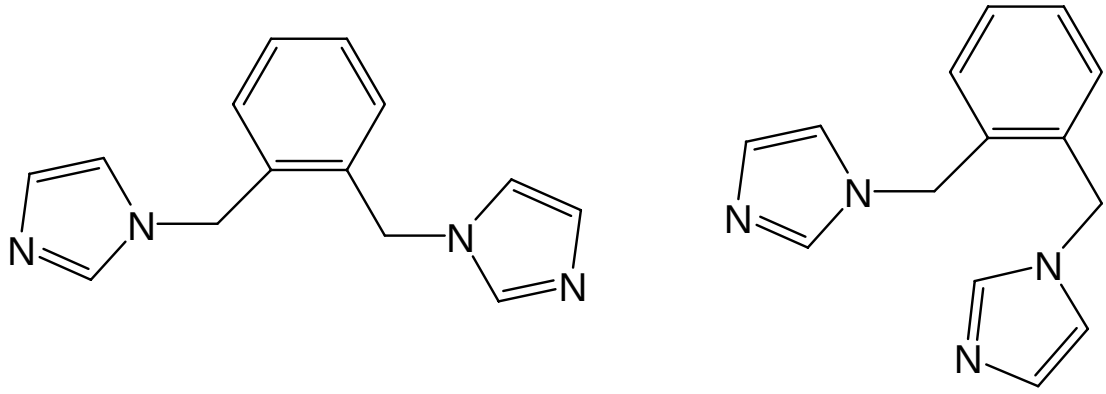

Scheme S1. The *trans*- and *cis*- conformations of the 1,2-bix ligands in **α** and **β**.

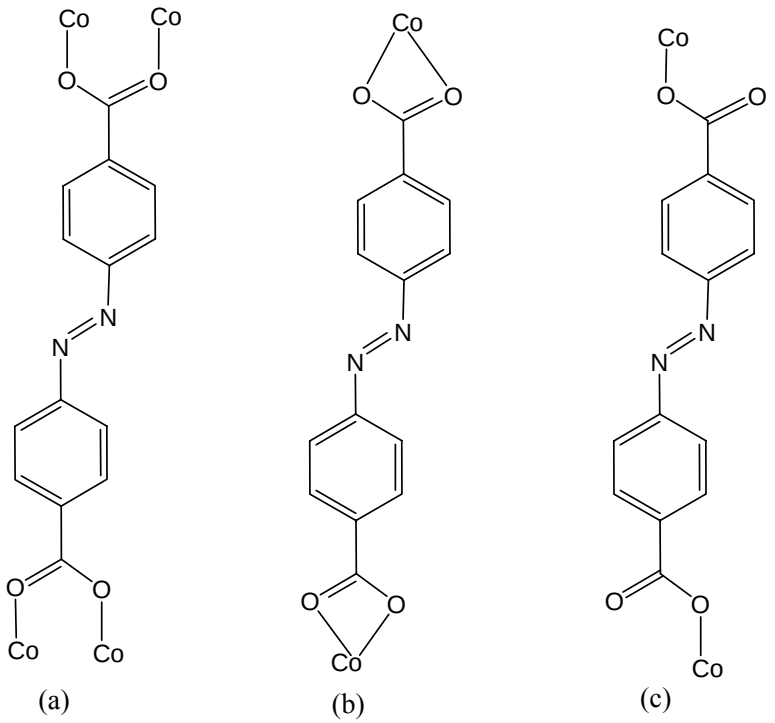

Scheme S2. The coordination modes of the L anions [(a) and (b) for **α** and (c) for **β**].

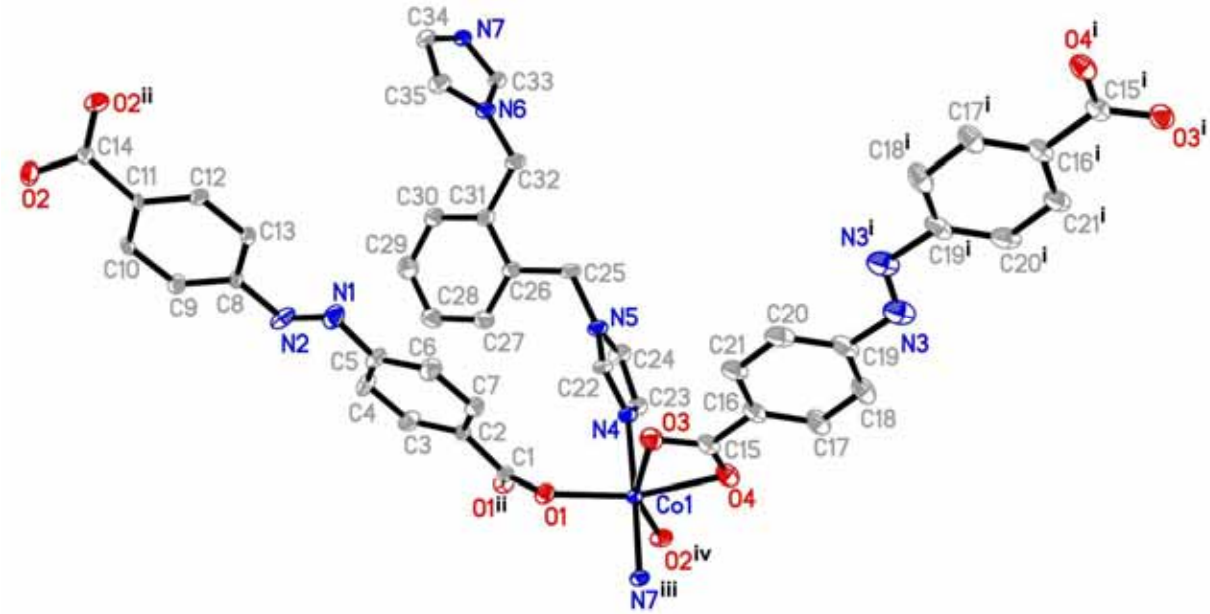

Fig. S7. The ORTEP figure of **α** (site occupation factors for C1-C14, N1 and N2 atoms are 0.5). Symmetry codes: (i) 1.5-x, 0.5-y, 2-z; (ii) 1-x, y, 0.5-z; (iii) x-0.5, y-0.5, z; (iv) 1-x, y-1, 0.5-z.

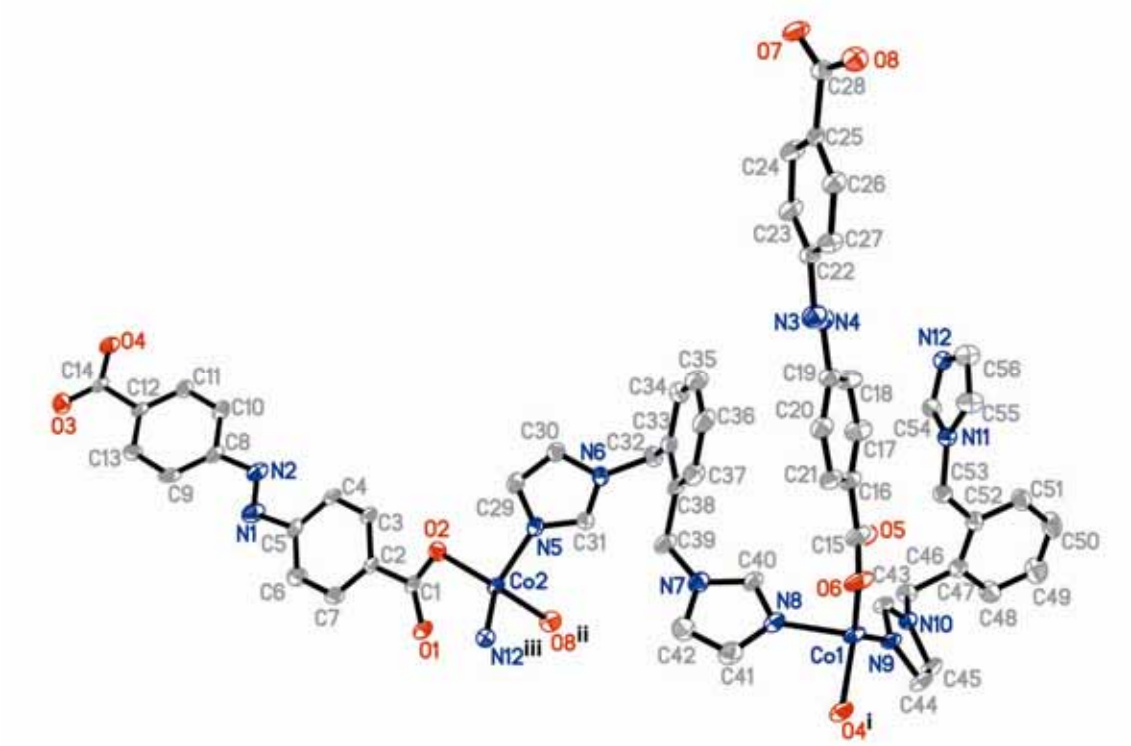

Fig. S8. The ORTEP figure of **β**. Symmetry codes: (i) 1.5+x, 0.5-y, 0.5+z; (ii) 0.5+x, 1.5-y, z-0.5; (iii) x, y-1, z.

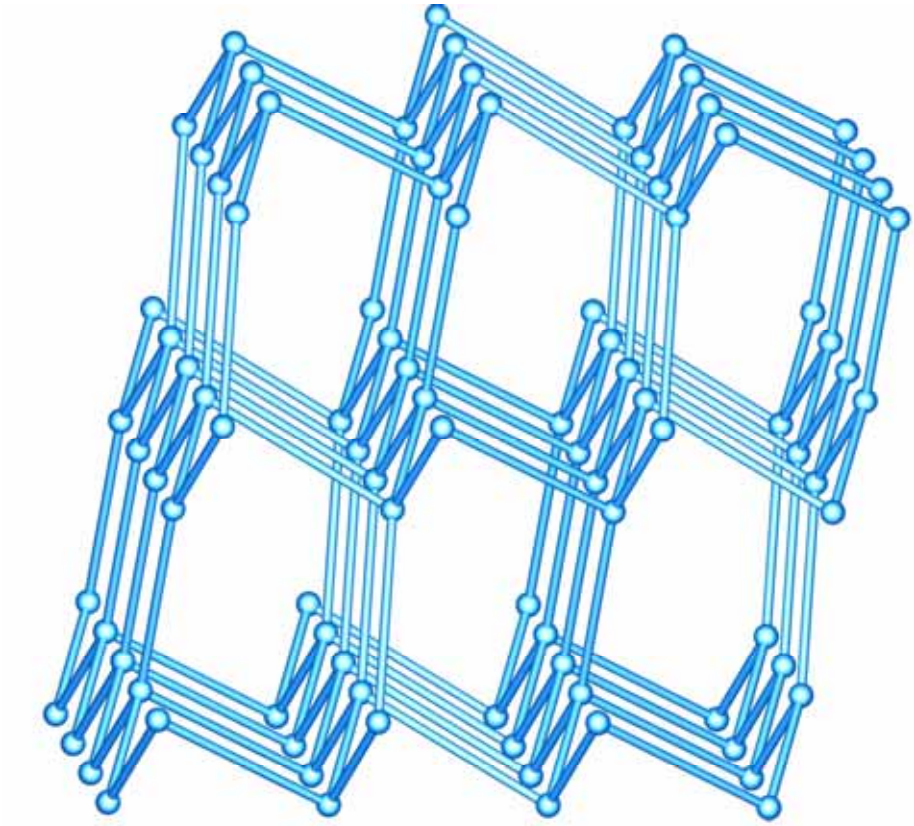

Fig. S9. The 4-connected $6^5.8$ topology of **β**.

Structural difference between β and cds net:

Although the structures of **β** and **cds** have the same Schläfli symbol ($6^5.8$), there are differences in their net geometries.

Fig. S10 shows the ideal **cds** net. After selecting a node (all nodes are equivalent), marked in red, we then selected the pair of links from that node that give the 8-membered shortest circuits (all the rest of the shortest circuits are 6-membered). We then marked out in green in the figure (apart from one yellow node which will be explained later) the two 8-membered rings that are possible with this pair of links. This leaves just two other links radiating out from the red node – these are part of 6-membered shortest circuits. Again, there are two possible ones; we have marked these out in blue (and black) in the figure. For each of the two blue 6-membered rings we have marked in black the node in each that is farthest away from the starting red node. The shortest pathway between these nodes not involving any nodes in the blue rings is the five yellow nodes marked in the figure. Note that one of the nodes in this yellow pathway is part of one of the green 8-membered rings discussed earlier.

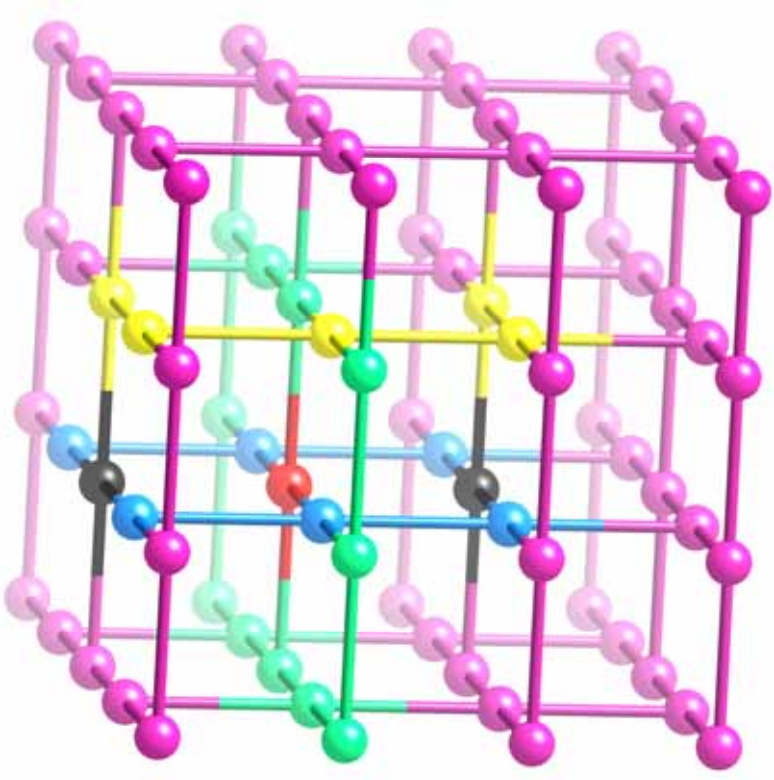

Fig. S10. The 4-connected **cds** net.

The same process was applied to the network of **β** (Fig. S11). A node (marked in red) was selected (all nodes are topologically equivalent even though there are two crystallographically), and we then selected the pair of links from this node that give the 8-membered shortest circuits (again, all the rest of the shortest circuits are 6-membered). We then marked out in green in the figure the two 8-membered rings that are possible with this pair of links. This leaves just two other links radiating out from the red node – as before, these are part of 6-membered shortest circuits. Again, there are two possible ones; we have marked these out in blue (and black) in the figure. For each of the two blue 6-membered rings we have marked in black the node in each that is farthest away from the starting red node. The shortest pathway between these nodes not involving any nodes in the blue rings is the five yellow nodes marked in the figure. Note that now, unlike the **cds** net described above, none of the nodes in this yellow pathway is part of one of the green 8-membered rings defined earlier. Therefore the two topologies are different.

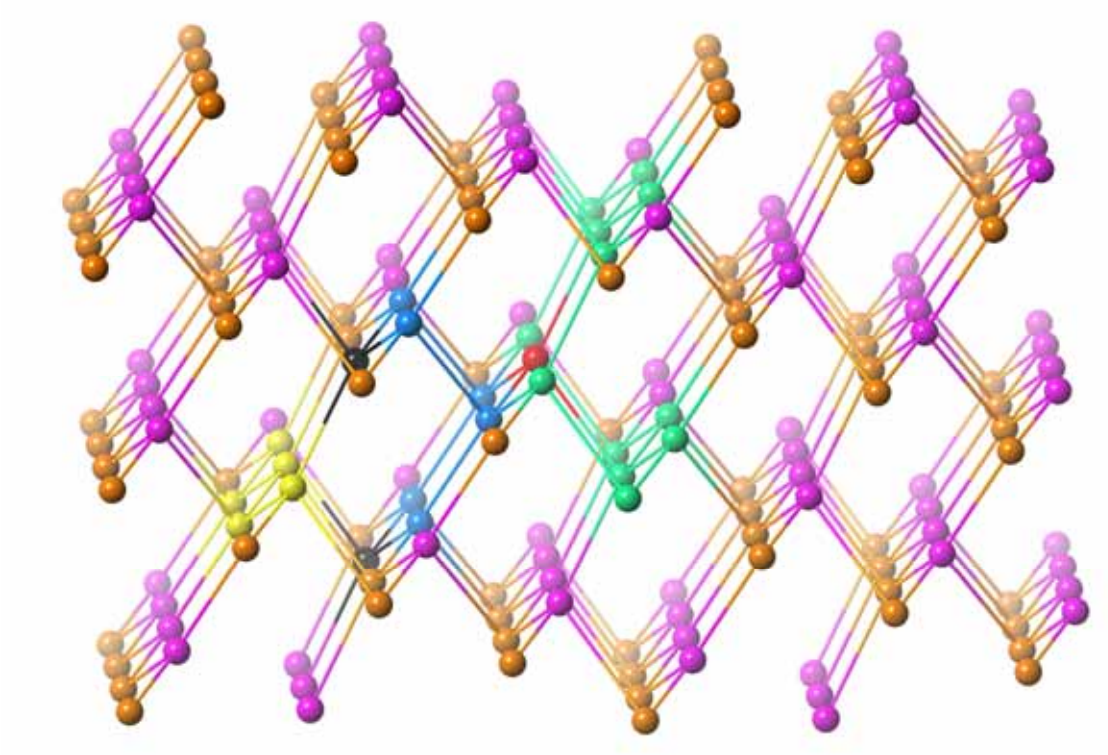

Fig. S11. The 4-connected $6^5.8$ topology of **β**.